



**HAL**  
open science

## Underwater Adhesion of Multiresponsive Complex Coacervates

Marco Dompé, Francisco J Cedano-Serrano, Mehdi Vahdati, Larissa van Westerveld, Dominique Hourdet, Costantino Creton, Jasper van Der Gucht, Thomas Kodger, Marleen Kamperman

► **To cite this version:**

Marco Dompé, Francisco J Cedano-Serrano, Mehdi Vahdati, Larissa van Westerveld, Dominique Hourdet, et al.. Underwater Adhesion of Multiresponsive Complex Coacervates. *Advanced Materials Interfaces*, In press, 10.1002/admi.201901785 . hal-02430667

**HAL Id: hal-02430667**

**<https://hal.sorbonne-universite.fr/hal-02430667>**

Submitted on 7 Jan 2020

**HAL** is a multi-disciplinary open access archive for the deposit and dissemination of scientific research documents, whether they are published or not. The documents may come from teaching and research institutions in France or abroad, or from public or private research centers.

L'archive ouverte pluridisciplinaire **HAL**, est destinée au dépôt et à la diffusion de documents scientifiques de niveau recherche, publiés ou non, émanant des établissements d'enseignement et de recherche français ou étrangers, des laboratoires publics ou privés.

# Underwater Adhesion of Multiresponsive Complex Coacervates

Marco Dompé, Francisco J. Cedano-Serrano, Mehdi Vahdati, Larissa van Westerveld, Dominique Hourdet, Costantino Creton, Jasper van der Gucht, Thomas Kodger, and Marleen Kamperman\*

Many marine organisms have developed adhesives that are able to bond under water, overcoming the challenges associated with wet adhesion. A key element in the processing of several natural underwater glues is complex coacervation, a liquid–liquid phase separation driven by complexation of oppositely charged macromolecules. Inspired by these examples, the development of a fully synthetic complex coacervate-based adhesive is reported with an in situ setting mechanism, which can be triggered by a change in temperature and/or a change in ionic strength. The adhesive consists of a matrix of oppositely charged polyelectrolytes that are modified with thermoresponsive poly(*N*-isopropylacrylamide) (PNIPAM) grafts. The adhesive, which initially starts out as a fluid complex coacervate with limited adhesion at room temperature and high ionic strength, transitions into a viscoelastic solid upon an increase in temperature and/or a decrease in the salt concentration of the environment. Consequently, the thermoresponsive chains self-associate into hydrophobic domains and/or the polyelectrolyte matrix contracts, without inducing any macroscopic shrinking. The presence of PNIPAM favors energy dissipation by softening the material and by allowing crack blunting. The high work of adhesion, the gelation kinetics, and the easy tunability of the system make it a potential candidate for soft tissue adhesion in physiological environments.

Adhesion in wet and dynamic environments represents a technological challenge, mainly because of the presence of water, which dramatically reduces the performance of commercially available adhesives.<sup>[1]</sup> Currently, no tissue adhesive has been approved for clinical use that complies with all the requirements, including: easy delivery, fast setting time, strong adhesive and cohesive properties, and biocompatibility.<sup>[2,3]</sup> Due to these difficulties, in medicine, adhesive technology has been applied primarily for stopping bleeding and gluing skin exter-

nally, while surgical tissue closure and sealing are exclusively performed with sutures and staples.<sup>[2]</sup> These conventional techniques have several drawbacks such as tissue damage, extension of operating times, and challenging application.<sup>[4,5]</sup> The development of effective surgical glues would dramatically reduce the incidence of such complications. Currently, glues designed for clinical applications have significant limitations: polycyanoacrylate glues induce inflammatory responses,<sup>[6]</sup> fibrin glues exhibit poor performances due to poor cohesive properties,<sup>[7]</sup> and other adhesives under development covalently react with functional groups at the tissue surface, becoming ineffective in the presence of blood.<sup>[8]</sup> Major efforts are underway to create new concepts, recently resulting in promising developments, such as bioinspired glues,<sup>[9–11]</sup> TisuGlu,<sup>[12]</sup> Gecko Biomedical GB02,<sup>[13]</sup> and silica nanoparticle suspensions.<sup>[14]</sup>

A different, largely unexplored, strategy for the development of surgical glues is based on complex coacervation,<sup>[15–21]</sup> which is involved in the processing of natural adhesives employed by several organisms to attach to different surfaces underwater.<sup>[22–24]</sup> Complex coacervates are polymer-rich, water-insoluble complexes of oppositely charged polyelectrolytes with a low surface tension that makes them compliant with surfaces.<sup>[25,26]</sup> After delivery, additional interactions need to be introduced to transition the viscous liquid into a strong and tough material to prevent flow under an applied stress.<sup>[27]</sup>

M. Dompé, Prof. J. van der Gucht, Dr. T. Kodger, Prof. M. Kamperman  
 Laboratory of Physical Chemistry and Soft Matter  
 Wageningen University and Research  
 Stippeneng 4, 6708 WE Wageningen, The Netherlands  
 E-mail: marleen.kamperman@rug.nl

 The ORCID identification number(s) for the author(s) of this article can be found under <https://doi.org/10.1002/admi.201901785>.

© 2019 The Authors. Published by WILEY-VCH Verlag GmbH & Co. KGaA, Weinheim. This is an open access article under the terms of the Creative Commons Attribution-NonCommercial License, which permits use, distribution and reproduction in any medium, provided the original work is properly cited and is not used for commercial purposes.

Dr. F. J. Cedano-Serrano, Dr. M. Vahdati, Prof. D. Hourdet,  
 Prof. C. Creton  
 Soft Matter Sciences and Engineering  
 ESPCI Paris  
 PSL University  
 Sorbonne University  
 CNRS  
 F-75005 Paris, France

L. van Westerveld, Prof. M. Kamperman  
 Polymer Science  
 Zernike Institute for Advanced Materials  
 University of Groningen  
 Nijenborgh 4, 9747 AG Groningen, The Netherlands

DOI: 10.1002/admi.201901785

Complex coacervation is thermodynamically regulated by a subtle balance between the entropy associated with the release of counterions bound to the polymer chains and the enthalpy of formation of new interpolyelectrolyte ion pairs.<sup>[25]</sup> This equilibrium strongly depends on ionic strength,  $I$ : at low salt concentration, complexation is generally favored but, by increasing  $I$ , the entropic gain decreases, meaning that above a critical salt concentration (CSC), phase separation does not occur and one-phase molecular solutions are obtained instead. Below the CSC, the mechanical properties can be tuned by choosing the appropriate salt concentration: the higher the  $I$ , the weaker are the electrostatic interactions keeping together the complex coacervate phase, which is therefore more mechanically compliant.<sup>[28]</sup> Consequently, by decreasing  $I$ , polyelectrolyte mixtures can result in materials spanning from viscoelastic liquids to solid complexes.<sup>[29,30]</sup>

In a previous work,<sup>[31]</sup> we have reported the development of a fully synthetic complex coacervate-based adhesive with a setting mechanism activated by a change in temperature. The adhesive formulation is obtained by mixing oppositely charged polyelectrolytes bearing thermoresponsive poly(*N*-isopropylacrylamide) (PNIPAM) chains at an added salt concentration just below the CSC, in order to obtain a fluid complex coacervate phase of low viscosity but still separated from water before injection. The adhesive shows a liquid-to-solid transition when only performing a *temperature switch*, resulting in a huge change in viscosity: by raising the temperature above the PNIPAM lower critical solution temperature (LCST, 23 °C at this  $I$ ) in an aqueous medium prepared at the same salt concentration, the complex coacervate is able to attach to different surfaces, regardless of their charge or hydrophobicity. However, after application, the final cohesive properties are mainly controlled by the formation of PNIPAM nodes, while the electrostatic interactions between the polyelectrolyte domains are not employed to effectively reinforce the material because of the constantly high  $I$  at all temperatures.

In this work, we report the introduction of an additional trigger, defined as *salt switch*, which enables the activation of the electrostatic interactions in the PNIPAM-functionalized complex coacervate. To achieve this, we test the adhesive performance in an aqueous environment prepared at a much lower  $I$ . The material undergoes a liquid-to-solid transition, which is only ascribed to the formation of stronger electrostatic interactions between the polyelectrolyte backbones while the thermoresponsive domains remain *dormant* because the temperature of the surrounding environment is kept below the LCST. Careful control of the salt concentration is therefore crucial both in the preparation and in the testing stage to tune the material properties. Furthermore, the combination of both salt and temperature switch, and the order in which they are applied, provide even more room to control the mechanical and the adhesive properties of the system.

This is the first report that systematically addresses the effect of a well-defined salt concentration gradient on the underwater adhesive properties of a synthetic system, although other research groups have already used ionic strength as a trigger to activate electrostatic interactions in wet environments.<sup>[32,33]</sup> Furthermore, the presence, within the same material, of polyelectrolyte chains and thermoresponsive domains, which can be independently activated by two different triggers, separates

the contribution of each hardening mechanism to the overall adhesive performance.

The PNIPAM-functionalized complex coacervates are obtained by mixing two oppositely charged graft copolymer solutions, namely poly(acrylic acid)-*grafted*-poly(*N*-isopropylacrylamide) (PAA-*g*-PNIPAM)<sup>[34]</sup> and poly(dimethylaminopropyl acrylamide)-*grafted*-poly(*N*-isopropylacrylamide) (PDMA-PAA-*g*-PNIPAM)<sup>[35]</sup> and their properties are compared to the properties of homopolymer (PNIPAM-free) complex coacervates (obtained by mixing homopolymer PAA and PDMA-PAA solutions) (Table S1, Supporting Information). The copolymers, whose synthesis has been reported in detail in our previous paper,<sup>[31]</sup> have a high molecular weight ( $M_n$  PAA-*g*-PNIPAM  $\approx$  400 kg mol<sup>-1</sup>,  $M_n$  PDMA-PAA-*g*-PNIPAM  $\approx$  250 kg mol<sup>-1</sup>) and a similar molar ratio of charged and NIPAM monomers ( $\approx$ 70:30).

The complex coacervate phase, initially prepared at an added salt concentration (0.75 M NaCl) close to the CSC (0.8 M NaCl), is injected into a lower  $I$  (0.1 M NaCl) medium at pH 7.0 (Figure 1A,B). The salt ions diffuse out of the adhesive, allowing the formation of stronger electrostatic interactions between oppositely charged polyelectrolyte chains. The evolution of the storage ( $G'$ ) and loss ( $G''$ ) moduli upon an in situ salt switch can be monitored via linear rheology. The material, initially a viscoelastic liquid ( $G' < G''$ ), turns immediately into a soft polyelectrolyte gel ( $G' > G''$ ) upon contact with a 0.1 M NaCl water solution and 20 °C (Figure 1C). In both homopolymer and graft copolymer complex coacervates, an abrupt increase in  $G'$  is observed within the first 10 min. After this period, the moduli tend toward a plateau, indicating that the ion diffusion process is finished by the end of the experiment.

A crucial parameter affecting the final adhesive performance is the water content (Figure 2A and Table S2, Supporting Information). During the salt switch, the water content may change and affect the material properties: swelling may lead to mechanical weakening,<sup>[10]</sup> while shrinking might favor the release of water at the interface, preventing an effective contact.<sup>[22]</sup> The water content is determined by thermogravimetric analysis (Figure S1, Supporting Information). Before the switch, at high salt concentration (0.75 M NaCl), the graft copolymer complex coacervates have a higher water content (91%) than the homopolymer complex coacervates (84%) because of the presence of the hydrophilic PNIPAM chains, which allows a higher water retention. The water content of the complex coacervate phase is generally known to decrease when reducing the salt concentration.<sup>[36]</sup> Here, in both graft and homopolymer complex coacervates, we observe a very slight increase in water content upon application of a salt switch, in line with other literature data.<sup>[37]</sup>

The water content, relatively speaking, increases because of the diffusion of the salt ions out of the complex coacervate phase. However, the total mass of water actually decreases, with graft copolymer complex coacervates losing 17.6% of the initial water mass and homopolymer complex coacervates losing 22.2% of the initial water mass. The higher water retention observed in graft copolymer complex coacervates might be ascribed to the presence of the hydrophilic PNIPAM units.

Additionally, the swelling ratio  $Q$  is equal to  $-19.6\%$  for graft copolymer complex coacervates and  $-23.4\%$  for homopolymer complex coacervates: the negative signs indicate that, in both cases, the total weight of the complex coacervate decreases, suggesting shrinkage of the sample. Crucially, these data are

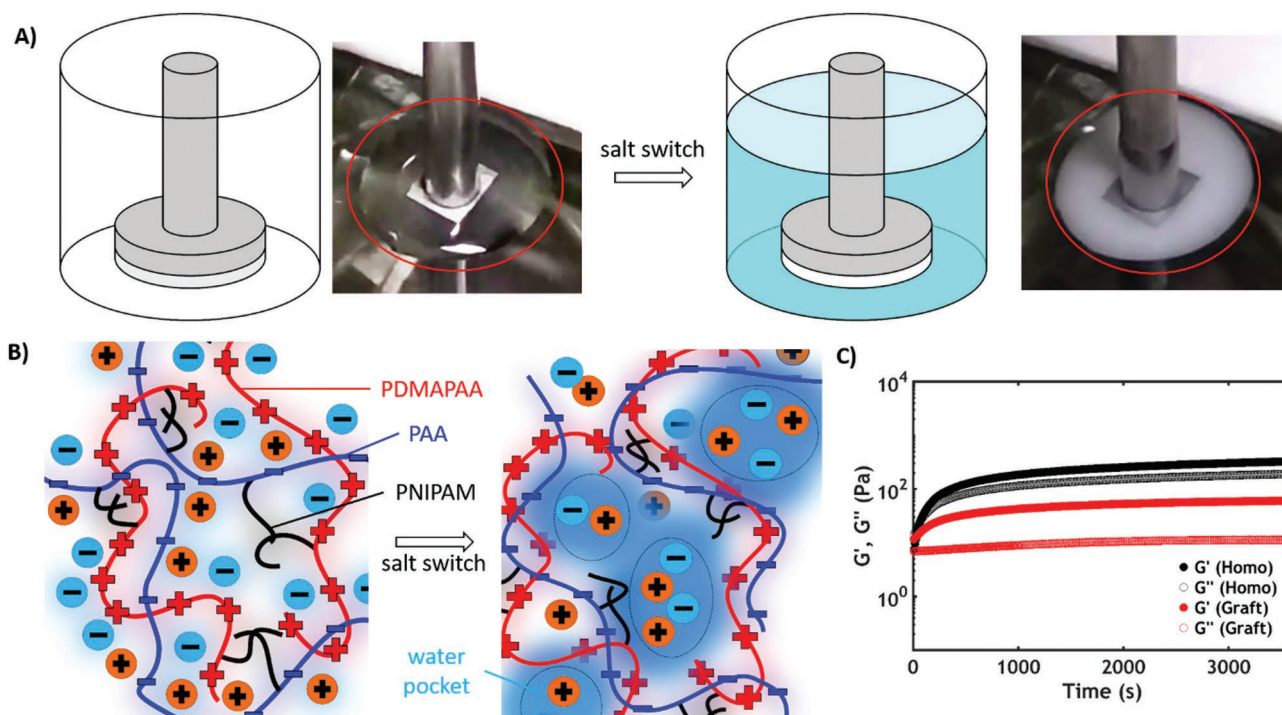


**Figure 1.** Illustration of the salt-triggered setting mechanism. A) Schematic and pictures of the adhesive setting: the material transitions from a transparent viscous liquid to a white soft gel. B) Schematic representation of the salt ion diffusion out of the graft copolymer complex coacervate phase: before the salt switch (left), the counterions are mostly bound to the polyelectrolyte chains and the adhesive has the features of a viscous liquid; after (right), the interactions between polyelectrolytes get stronger and counterions are expelled in water pockets. C) Evolution of  $G'$  and  $G''$  during setting at a fixed frequency of  $0.1 \text{ rad s}^{-1}$  and at a temperature of  $20 \text{ }^\circ\text{C}$ .

obtained when the samples are not confined in a particular geometry but only soaked in the aqueous medium: however, no obvious macroscopic change in volume is visible by eye when confining the adhesive between two glass slides (layer thickness =  $0.05 \text{ mm}$ ). Furthermore, no significant variation of the normal force (Figure S2, Supporting Information) is detected when following the setting with a rheometer, meaning that the transition occurs with negligible volume change and, most likely, with higher water retention when compared to the unconfined sample. This might also be ascribed to the fact that phase separation occurs in a confined environment where the complex fluid already adheres, even weakly, to the surface.

Additionally, when performing a salt switch, the complex coacervate phase is brought out of equilibrium. Indeed, homopolymer complex coacervates prepared at  $0.1 \text{ M NaCl}$  show a water content equal to  $63.8\%$  and a polymer content equal to  $32.1\%$ , in accordance with other literature data.<sup>[36]</sup> According to thermodynamics, when performing a salt switch,  $Q$  should then be equal to  $-70.4\%$  and the amount of released water should be  $77.6\%$  of the initial water mass. However the values here recorded are much lower, indicating that most of the water is retained by the complex coacervate: as shown in similar work performed on polyelectrolyte complexes,<sup>[37]</sup> the exposure to a lower  $I$  environment may lead to a sudden contraction of the polyelectrolyte matrix, leading to the formation of a kinetically arrested state, with most of the water remaining trapped in pores within the material (Figure 1B). The presence of a porous structure in this system has been already detected

using optical microscopy in previous work<sup>[31]</sup> and shown here as Figure S5 in the Supporting Information: both observations are in accordance with other reports about complex coacervates and polyelectrolyte complexes.<sup>[15,37,38]</sup>

As previously mentioned, the salt-triggered setting mechanism is driven by the ion diffusion out of the complex coacervate phase.<sup>[39]</sup> In order to determine the end of the transition, the adhesive is loaded into a glass container which is part of a custom-made adhesion setup allowing visualization from the bottom (Figure S6, Supporting Information). As preload is impossible due to the viscous nature of the sample which relaxes over time, contact with a mica probe is performed imposing a final adhesive thickness of  $0.2 \text{ mm}$ . After pouring the  $0.1 \text{ M NaCl}$  solution into the container, the adhesive setting is imaged directly. As shown in Figure 2B, the complex coacervate phase, initially transparent, gradually turns white: the growing opacity is attributed to the resulting scattering from the formation of water-filled pores, which have a different refracting index compared to the densifying polyelectrolyte complex.<sup>[38]</sup> The change in opacity is immediate at the edges of the sample, where the material is in direct contact with the surrounding medium, and progressively develops toward the center of the complex coacervate phase.

In line with similar experiments,<sup>[39]</sup> the whole transition visually takes  $\approx 45 \text{ min}$ , both in graft copolymer and in homopolymer complex coacervates, while, mechanically, according to the rheology data, the moduli, after a dramatic increase in the first  $10 \text{ min}$  (Figure S3, Supporting Information), head toward

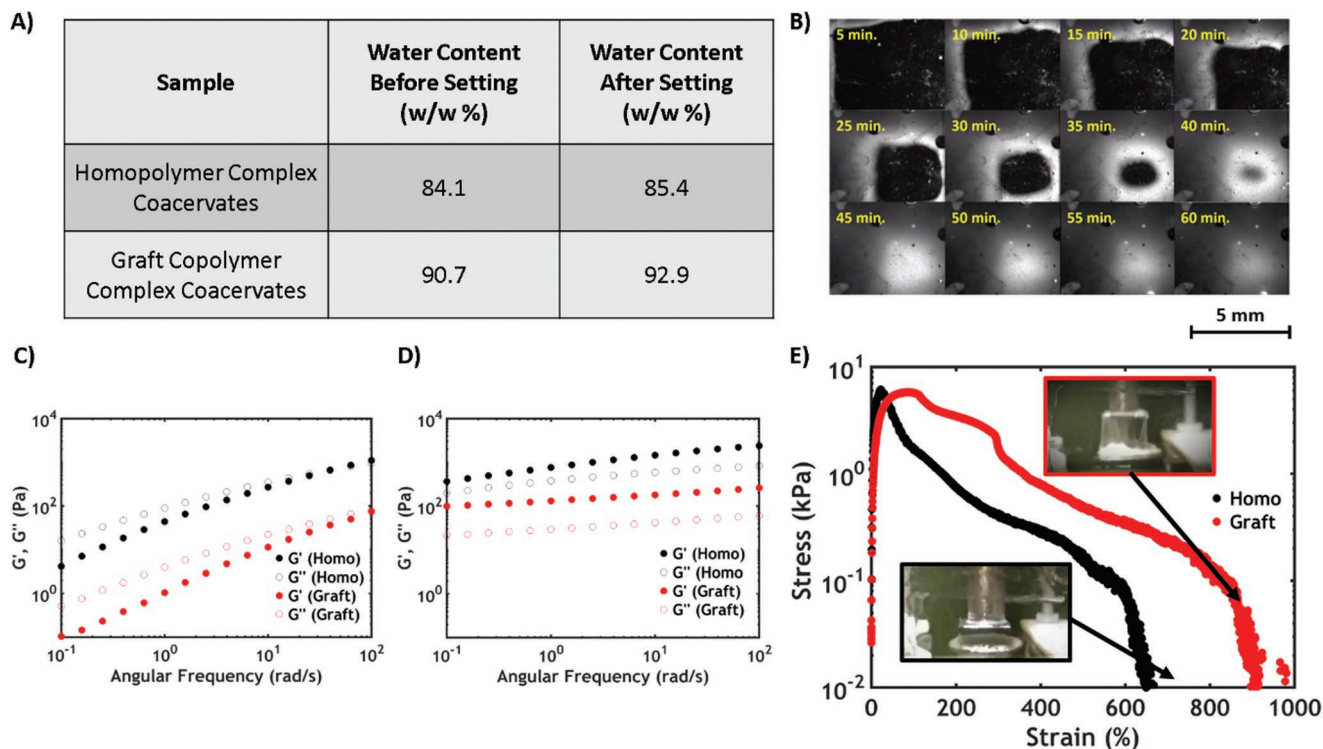


**Figure 2.** Mechanical and adhesive properties of homopolymer and graft copolymer complex coacervates in response to a salt-triggered setting process. A) Water content data before and after the setting process. B) In-time visualization of the adhesive setting in homopolymer complex coacervates from the bottom of the setup. C) Frequency sweeps performed on both material systems before and D) after the salt switch. E) Underwater adhesive performance of both material systems. In the insets the different modes of failure for homopolymer (black) and graft copolymer (red) complex coacervates are shown.

a plateau. However, when plotted in a lin–lin scale (Figure S4, Supporting Information), it is observed that the moduli still increase at longer times, albeit with a slower pace. Initially, diffusion is fast because the sample is liquid: the abrupt increase in moduli by more than an order of magnitude at the beginning of the experiment is due to the formation of solid regions at the edges of the sample, which coexist with liquid zones and which dominate the average moduli. This leads to the formation of a dense layer that acts as a barrier for further diffusion. As this barrier grows, diffusion slows down further and the slope of the modulus–time curve decreases. The visualization of the transition is therefore essential to determine the contact time required for the complete setting: a homogeneous solid material will perform much better than a heterogeneous one, in which the liquid regions, unable to offer any resistance to applied stress, act as defects, facilitating crack propagation within the system. Since no further variation is observed after 45 min, a contact time of 1 h is set as standard for all the experiments described hereafter.

At high salt concentration, both homopolymer and graft copolymer complex coacervates show typical features of a viscous liquid (Figure 2C), with  $G''$  higher than  $G'$  over almost the whole range of frequencies: the chains can slide along each other with transient electrostatic interactions, with macroion pairs acting as sticky points.<sup>[28]</sup> After setting, both moduli become almost frequency independent, with  $G'$  exceeding  $G''$  (Figure 2D): the formation of stronger electrostatic interactions

slows down the chain dynamics, strengthening the material considerably and leading to the formation of a solid-like network.<sup>[40]</sup> Before and after the transition, the moduli are higher in the homopolymer complex coacervates because of the lower water content and thus a higher concentration of sticky points:  $G' \approx Nk_B T$ , where  $N$  is the number of elastically active chain segments per unit volume.<sup>[41]</sup> Since the presence of PNIPAM units favors water retention, resulting in a lower concentration of crosslinking units, it follows that the copolymer composition has a profound effect in defining the moduli of the adhesive. In addition to that, the complex viscosity ( $\eta^*$ ) measured at low frequency (0.1 rad s<sup>-1</sup>) and at 0.75 M NaCl is much lower in graft copolymer complex coacervates (5.28 Pa s) compared to the homopolymer counterpart (165 Pa s). This indicates that, when developing a soft tissue adhesive, the incorporation of the PNIPAM side chains, together with a high  $I$ , facilitates injectability.

Underwater adhesion experiments are conducted using a probe-tack test with the setup developed by Sudre et al.<sup>[42]</sup> and using the technique reported in our previous work.<sup>[31]</sup> Contact is made between the fluid complex coacervate phase and a negatively charged PAA hydrogel thin film (dry thickness = 144 nm), attached on the probe surface, until a fixed thickness of the complex coacervate layer of 0.5 mm is reached. A 0.1 M NaCl water solution at a fixed temperature of 20 °C is then added in the chamber (Figure 1A). After 1 h contact time (no significant difference in adhesion performance is detected at longer

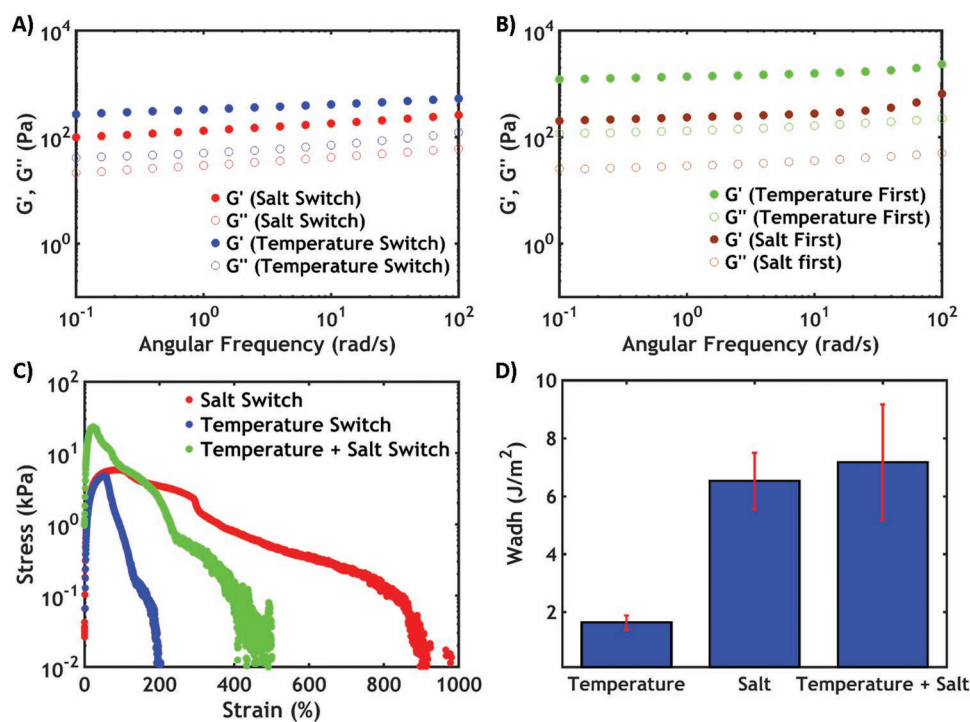


**Figure 3.** Mechanical and adhesive behavior of the graft copolymer complex coacervate phase in response to different triggers. A) Frequency sweeps obtained after either a temperature or a salt switch. B) Effect of the history of the setting process on the rheological properties when applying a combined temperature and salt trigger. C) Adhesion performance and D) work of adhesion measured after different environmentally triggered setting processes.

times, as shown in Figure S7, Supporting Information), the probe is pulled off at a velocity of  $100 \mu\text{m s}^{-1}$  corresponding to a nominal strain rate of  $0.2 \text{ s}^{-1}$ .

A good balance between elastic modulus, interfacial interactions, and viscoelastic dissipation (controlling adhesion) is required to optimize the adhesive performance.<sup>[43]</sup> Both homopolymer and graft copolymer complex coacervates show that balance and fail by crack blunting and fibril formation (Figure 2E). However, the homopolymer complex coacervate eventually fails adhesively, without leaving any residues on the probe suggesting a strain hardening mechanism active in extension at large strain (Figure 2E, black inset),<sup>[43]</sup> with a work of adhesion ( $W_{adh}$ ) equal to  $3.2 \text{ J m}^{-2}$ . For the graft copolymer complex coacervate, a better performance ( $W_{adh} = 6.5 \text{ J m}^{-2}$ ) is obtained: the presence of the PNIPAM chains favors water retention, thereby rendering the material softer and most likely suppressing the strain hardening at large strain. This leads to an increased deformability and dissipation which results in more stable fibrils and a higher extension at break: as a result, the material fails cohesively, leaving residues on the detaching surface (Figure 2E, red inset).<sup>[44,45]</sup> Finally, we have shown, in our previous work,<sup>[31]</sup> that PNIPAM side chains already self-associate below the LCST: the slight increase in toughness may also be ascribed to the presence of different types of noncovalent interactions leading to a variety of bond strengths.<sup>[46]</sup> The recorded work of adhesion values are in line with the values measured for other biomimetic adhesives tested with an underwater probe-tack setup in similar conditions ( $0.5\text{--}6.5 \text{ J m}^{-2}$ ),<sup>[47,48]</sup> and somewhat

higher than the values detected for commercial pressure sensitive adhesives measured underwater ( $2 \text{ J m}^{-2}$ ).<sup>[49]</sup>

As is generally the case,<sup>[44]</sup> the work of adhesion increases as a function of the applied probe retraction rate. More interestingly,  $W_{adh}$  is always higher in graft copolymer complex coacervates as compared to homopolymer complex coacervates (Figure S8, Supporting Information). At greater detachment speeds, molecular friction is higher and more energy gets dissipated. While in PNIPAM-reinforced complex coacervates the mode of failure (adhesive or cohesive) does not change with the applied strain rate, in homopolymer complex coacervates it is possible to observe a transition from an adhesive to a cohesive mode of failure (Figure S9, Supporting Information) if the detachment is performed at a very low strain rate ( $0.002 \text{ s}^{-1}$ ); this is a further evidence that in such a viscoelastic material the adhesive performance is greatly affected by the applied strain rate.

The graft copolymer complex coacervates can be triggered by either temperature or salt, or by both. Despite the differently activated interactions, the moduli measured at the end of the two transitions have similar values, being slightly higher after a temperature switch (Figure 3A):  $G'$  exceeds  $G''$  over the whole range of frequencies, indicating in both cases the formation of a soft elastic gel. The number of PNIPAM nodes formed after a temperature switch is slightly higher than the amount of sticky points present after a salt switch: however, this should strongly depend on the molar ratio between thermoresponsive and polyelectrolyte moieties and the situation is expected to be reversed at a lower PNIPAM content.

Despite the similarities in linear rheological properties, the work of adhesion obtained after performing a salt switch ( $6.5 \text{ J m}^{-2}$ ) is much higher than the one reached after a temperature switch ( $1.6 \text{ J m}^{-2}$ ) (Figure 3D). While the cohesive mode of failure is similar, after a salt switch the adhesive can be stretched to a maximum strain which is almost five times higher than after a temperature switch (Figure 3C). The architecture and the composition of the polymers used might play a key role here: the graft copolymers synthesized have long polyelectrolyte backbones ( $M_n \approx 200 \text{ kg mol}^{-1}$ ) bearing short PNIPAM side chains ( $M_n \approx 5.5 \text{ kg mol}^{-1}$ ), with the molar ratio between charged units and thermoresponsive chains being 70:30. When performing a temperature switch, the short PNIPAM units, with restricted mobility as they are covalently attached to the main chain, are collapsed forming small domains, which will be therefore broken apart at a relatively small strain. However, when performing a salt switch, the adhesive needs to be stretched much more in order to completely disentangle the polyelectrolyte backbones due to their higher molecular weight than the PNIPAM chains. Similar observations were reported by Guo et al. when exploring the effect of the architecture of PNIPAM-based hydrogels on fracture properties,<sup>[50]</sup> highlighting that the microphase separated structure has a dramatic impact on large strain behavior.

Additionally, the change in salt concentration might also affect the adhesive interactions with the probe, which consists of a poly(acrylic acid) hydrogel thin film, that is negatively charged at the pH used in this study. At a lower  $I$ , the electrostatic interactions between the probe and the charged domains in the complex coacervate get stronger. The improvement in work of adhesion, when compared to a temperature switch, might therefore also originate from stronger adhesive interactions with the probe.

Since the material combines polyelectrolyte components and thermoresponsive units, the material properties were also tested in response to a combined temperature-salt trigger. Interestingly, the order in which the switch is performed considerably affects the rheological properties (Figure 3B). If the salt switch is performed before the temperature switch, the moduli obtained reach the same values as the ones measured after a single salt switch. Conversely, if the temperature is raised above the LCST followed by the activation of the electrostatic interactions, the final moduli increase by an order of magnitude, with  $G'$  reaching values around 1 kPa. Again the polymer architecture is thought to considerably affect the final properties. If the salt switch is performed first, the short PNIPAM chains, stuck in a matrix of long collapsed polyelectrolyte units, may not have the required mobility to find each other and form strong interchain nodes: the concentration of sticky points and consequently the moduli are therefore the same as when performing a single salt switch. However, when the temperature switch is performed before the salt switch, the shorter PNIPAM chains, now mobile and dynamic, can collapse first and self-associate into hydrophobic domains bridging polymer chains. As such, the activation of the electrostatic interactions between the longer polyelectrolyte backbones leads to an overall increase of the number of crosslinking points per unit volume and, therefore, of the moduli.

Finally, the adhesive performance is tested after performing a combined temperature and salt switch (Figure 3C). After loading the adhesive between probe and substrate, a 0.1 M NaCl aqueous solution, preheated at  $50 \text{ }^\circ\text{C}$ , is added and after 1 h of contact the probe is retracted. Since the kinetics of the transition is different, this would be equivalent to test the temperature switch first (leading therefore to a higher number of physical interactions within the material): when the target temperature is reached, the collapse of the thermoresponsive chains occurs on a timescale on the order of seconds<sup>[51]</sup> and is homogeneously distributed throughout the material. On the other hand, during a salt switch only the regions in immediate proximity of the aqueous medium are quickly triggered, as shown in Figure 2A, while the complete transition requires a setting time spanning from 60 min, as observed in this system, up to 24 h.<sup>[32]</sup>

The adhesive fails again in a cohesive fashion, leaving residues on the probe, and the final work of adhesion is similar ( $7.2 \text{ J m}^{-2}$ ) to the one obtained after a salt switch ( $6.5 \text{ J m}^{-2}$ ) (Figure 3D). This means that the insertion of the PNIPAM chains would promote a suitable adhesion performance in biological environments, such as the human body, where the glue would experience both a gradient in temperature and ionic strength. Additionally, the combination of PNIPAM chains and polyelectrolyte domains allows more control over the whole setting process in such a complex environment.

In conclusion, we have shown that PNIPAM-reinforced coacervates provide a good underwater adhesion performance in response to different triggers. The adhesive exhibits a liquid-to-solid transition without the addition of any covalent crosslinking agent, but exclusively in response to a change in temperature and salt concentration of the surrounding environment. As the environmental conditions used in this study resemble the physiological conditions, we believe that the combination of electrostatic interactions and thermoresponsive units results in a material system with promising properties for injectable adhesives for soft tissue repair or wound closure: future work will be focused on further improving the mechanical properties and on testing the underwater adhesive performance on soft tissues.

## Supporting Information

Supporting Information is available from the Wiley Online Library or from the author.

## Acknowledgements

This project is part of the BioSmartTrainee Network. The project has received funding from the European Union's Horizon 2020 research and innovation programme under the Marie Skłodowska-Curie Grant Agreement No. 642861. J.v.d.G. acknowledges the European Research Council for financial support (ERC Consolidator grant Softbreak).

## Conflict of Interest

The authors declare no conflict of interest.

## Keywords

complex coacervation, environmentally triggered setting mechanism, poly(*N*-isopropylacrylamide), polyelectrolytes, underwater adhesion

Received: October 22, 2019

Revised: December 6, 2019

Published online:

- [1] J. H. Waite, *Int. J. Adhes. Adhes.* **1987**, *7*, 9.
- [2] P. J. M. Bouten, M. Zonjee, J. Bender, S. T. K. Yauw, H. van Goor, J. C. M. van Hest, R. Hoogenboom, *Prog. Polym. Sci.* **2014**, *39*, 1375.
- [3] A. I. Bochyńska, G. Hannink, R. Verhoeven, D. W. Grijpma, P. Buma, *J. Mater. Sci.: Mater. Med.* **2016**, *28*, 22.
- [4] A. P. Duarte, J. F. Coelho, J. C. Bordado, M. T. Cidade, M. H. Gil, *Prog. Polym. Sci.* **2012**, *37*, 1031.
- [5] A. L. Tajirian, D. J. Goldberg, *J. Cosmet. Laser Ther.* **2010**, *12*, 296.
- [6] B. J. Vote, M. J. Elder, *Clin. Exp. Ophthalmol.* **2000**, *28*, 437.
- [7] A. Lauto, D. Mawad, L. J. R. Foster, *J. Chem. Technol. Biotechnol.* **2008**, *83*, 464.
- [8] J. Li, A. D. Celiz, J. Yang, Q. Yang, I. Wamala, W. Whyte, B. R. Seo, N. V. Vasilyev, J. J. Vlassak, Z. Suo, D. J. Mooney, *Science* **2017**, *357*, 378.
- [9] Y. Lee, C. Xu, M. Sebastin, A. Lee, N. Holwell, C. Xu, D. Miranda Nieves, L. Mu, R. S. Langer, C. Lin, J. M. Karp, *Adv. Healthcare Mater.* **2015**, *4*, 2587.
- [10] D. G. Barrett, G. G. Bushnell, P. B. Messersmith, *Adv. Healthcare Mater.* **2013**, *2*, 745.
- [11] Y. Liu, H. Meng, Z. Qian, N. Fan, W. Choi, F. Zhao, B. P. Lee, *Angew. Chem., Int. Ed.* **2017**, *56*, 4224.
- [12] R. Ohlinger, L. Gieron, R. Rutkowski, T. Kohlmann, M. Zygmunt, J. Unger, *In vivo* **2018**, *32*, 625.
- [13] D. Wussler, S. Kiefer, J. Haberstrohm, N. Kessler, R. Kubicki, D. Ruh, C. Heilmann, A. Seifert, M. Siepe, B. Stiller, N. Lang, *Thorac. Cardiovasc. Surg.* **2016**, *64*, ePP106.
- [14] S. Rose, A. PrevotEAU, P. Elzière, D. Hourdet, A. Marcellan, L. Leibler, *Nature* **2013**, *505*, 382.
- [15] R. J. Stewart, C. S. Wang, H. Shao, *Adv. Colloid Interface Sci.* **2011**, *167*, 85.
- [16] H. Shao, R. J. Stewart, *Adv. Mater.* **2010**, *22*, 729.
- [17] S. Seo, S. Das, P. J. Zalicki, R. Mirshafian, C. D. Eisenbach, J. N. Israelachvili, J. H. Waite, B. K. Ahn, *J. Am. Chem. Soc.* **2015**, *137*, 9214.
- [18] Q. Zhao, D. W. Lee, B. K. Ahn, S. Seo, Y. Kaufman, J. N. Israelachvili, J. H. Waite, *Nat. Mater.* **2016**, *15*, 407.
- [19] B. K. Ahn, S. Das, R. Linstadt, Y. Kaufman, N. R. Martinez-Rodriguez, R. Mirshafian, E. Kesselman, Y. Talmon, B. H. Lipshutz, J. N. Israelachvili, J. H. Waite, **2015**, *6*, 8663.
- [20] D. S. Hwang, H. Zeng, A. Srivastava, D. V. Krogstad, M. Tirrell, J. N. Israelachvili, J. H. Waite, *Soft Matter* **2010**, *6*, 3232.
- [21] L. Zhang, V. Lipik, A. Miserez, *J. Mater. Chem. B* **2016**, *4*, 1544.
- [22] J. H. Waite, N. H. Andersen, S. Jewhurst, C. Sun, *J. Adhes.* **2005**, *81*, 297.
- [23] G. Walker, *Mar. Biol.* **1970**, *7*, 239.
- [24] R. J. Stewart, J. C. Weaver, D. E. Morse, J. H. Waite, *J. Exp. Biol.* **2004**, *207*, 4727.
- [25] J. v. d. Gucht, E. Spruijt, M. Lemmers, M. A. Cohen Stuart, *J. Colloid Interface Sci.* **2011**, *361*, 407.
- [26] E. Spruijt, J. Sprakel, M. A. Cohen Stuart, J. van der Gucht, *Soft Matter* **2010**, *6*, 172.
- [27] R. J. Stewart, C. S. Wang, I. T. Song, J. P. Jones, *Adv. Colloid Interface Sci.* **2017**, *239*, 88.
- [28] E. Spruijt, M. A. Cohen Stuart, J. van der Gucht, *Macromolecules* **2013**, *46*, 1633.
- [29] Q. Wang, J. B. Schlenoff, *Macromolecules* **2014**, *47*, 3108.
- [30] K. Sadman, Q. Wang, Y. Chen, B. Keshavarz, Z. Jiang, K. R. Shull, *Macromolecules* **2017**, *50*, 9417.
- [31] M. Dompé, F. J. Cedano-Serrano, O. Heckert, N. van den Heuvel, J. van der Gucht, Y. Tran, D. Hourdet, C. Creton, M. Kamperman, *Adv. Mater.* **2019**, *31*, 1808179.
- [32] J. P. Jones, M. Sima, R. G. O'Hara, R. J. Stewart, *Adv. Healthcare Mater.* **2016**, *5*, 795.
- [33] S. Kim, H. Y. Yoo, J. Huang, Y. Lee, S. Park, Y. Park, S. Jin, Y. M. Jung, H. Zeng, D. S. Hwang, Y. Jho, *ACS Nano* **2017**, *11*, 6764.
- [34] A. Durand, D. Hourdet, *Polymer* **1999**, *40*, 4941.
- [35] L. Petit, C. Karakasyan, N. Pantoustier, D. Hourdet, *Polymer* **2007**, *48*, 7098.
- [36] E. Spruijt, A. H. Westphal, J. W. Borst, M. A. Cohen Stuart, J. van der Gucht, *Macromolecules* **2010**, *43*, 6476.
- [37] C. H. Porcel, J. B. Schlenoff, *Biomacromolecules* **2009**, *10*, 2968.
- [38] H. H. Hariri, A. M. Lehaf, J. B. Schlenoff, *Macromolecules* **2012**, *45*, 9364.
- [39] R. A. Ghostine, R. F. Shamoun, J. B. Schlenoff, *Macromolecules* **2013**, *46*, 4089.
- [40] J. Courtois, I. Baroudi, N. Nouvel, E. Degrandi, S. Pensec, G. Ducouret, C. Chanéac, L. Bouteiller, C. Creton, *Adv. Funct. Mater.* **2010**, *20*, 1803.
- [41] P. J. Flory, *Principles of Polymer Chemistry*, Cornell University Press, Ithaca, NY **1953**.
- [42] G. Sudre, L. Olanier, Y. Tran, D. Hourdet, C. Creton, *Soft Matter* **2012**, *8*, 8184.
- [43] F. Deplace, C. Carelli, S. Mariot, H. Retsos, A. Chateauminois, K. Ouzineb, C. Creton, *J. Adhes.* **2009**, *85*, 18.
- [44] C. Creton, M. Ciccotti, *Rep. Prog. Phys.* **2016**, *79*, 046601.
- [45] C. Y. Hui, A. Jagota, S. J. Bannison, J. D. Londono, *Proc. R. Soc. London, Ser. A* **2003**, *459*, 1489.
- [46] T. L. Sun, T. Kurokawa, S. Kuroda, A. B. Ihsan, T. Akasaki, K. Sato, M. A. Haque, T. Nakajima, J. P. Gong, *Nat. Mater.* **2013**, *12*, 932.
- [47] H. Chung, P. Glass, J. M. Pothén, M. Sitti, N. R. Washburn, *Biomacromolecules* **2011**, *12*, 342.
- [48] M. Guvendiren, P. B. Messersmith, K. R. Shull, *Biomacromolecules* **2008**, *9*, 122.
- [49] S. K. Clancy, A. Sodano, D. J. Cunningham, S. S. Huang, P. J. Zalicki, S. Shin, B. K. Ahn, *Biomacromolecules* **2016**, *17*, 1869.
- [50] H. Guo, N. Sanson, D. Hourdet, A. Marcellan, *Adv. Mater.* **2016**, *28*, 5857.
- [51] J. Xu, Z. Zhu, S. Luo, C. Wu, S. Liu, *Phys. Rev. Lett.* **2006**, *96*, 027802.